Pramana – J. Phys., Vol. 39, No. 2, August 1992, pp. 117–130. © Printed in India.

Solid state effects during deuterium implantation into copper and titanium

H K SAHU, M C VALSAKUMAR, B PANIGRAHI, K G M NAIR and K KRISHAN

Materials Science Division, Indira Gandhi Centre for Atomic Research, Kalpakkam 603 102, India

MS received 10 February 1992

Abstract. Results of neutron counting experiments during deuterium implantation into titanium and copper are reported. Models for neutron yield have been developed by taking into account different solid state effects like energy degradation of incident ions, energy dependent d–d fusion cross section and diffusion of implanted deuterium possibly influenced by surface desorption and formation of metal deuterides. The asymptotic time dependence of the neutron yield during implantation has been compared with the experimental results. Using these results, solid state processes that might occur during deuterium implantation into these metals are inferred.

Keywords. Ion implantation; deuterium; titanium; copper; diffusion; desorption; hydride formation; d–d fusion.

PACS No. 66·30

1. Introduction

Hydrogen loaded metals have a large number of technological applications ranging from hydrogen storage to neutron moderation and shielding in nuclear reactors (Mueller 1968). Also on exposure to reactor environments some metals get loaded with gaseous transmutation products such as hydrogen, its isotopes and helium. Various properties of the metals are effected by the presence of these gases (Alefeld and Volkl 1978). The physical behavior of hydrogen and its isotopes in metals is different from that of helium because the migration of hydrogen is much faster. Further, varying degrees of the chemical affinity of different metals for hydrogen leads to a variety of situations. Moreover, recently there has been a lot of interest in deuterium loaded metals because of the observation (Jones *et al* 1989; Srinivasan 1991) of unusual "cold fusion phenomenon" occurring during deuterium charging.

This paper presents theoretical analysis of deuterium implantation experiment which uses ion implantation as the method for deuterium charging into foils of titanium and copper. In this experiment we are interested in measuring the fusion neutron yield as a function of time for a constant implantation energy and beam current. The neutron yield depends on the diffusion, desorption and formation of metal deuterides which influence the deuterium concentration profile of the implanted deuterium. Over and above the monotonic rise in neutron yield we have observed additional peak structures in the time dependence of the neutron yield. This we believe

arises from the increased d–d fusion cross section due to deuterium kinetics in the metal. However, in this paper we examine the time dependence of the neutron yield for these implantation conditions on the basis of known d–d fusion cross section data (Duane 1972).

As the implantation proceeds the deuterium concentration builds up inside the metal. The incident deuterons continuously interact with the implanted deuterium via the d–d fusion reaction. The neutron yield therefore carries the signature of the implanted deuterium concentration which in turn evolves in time influenced by the diffusion, formation of deuterides and surface desorption. The parameters of interest are the neutron counts N acquired during the interval t_m from $t = mT$ to $(m+1)T$ and the total neutron counts N_{tot} recorded up to time t. The asymptotic values of these variables have been found to follow power laws like t_m^a and t^b respectively. In this paper we will examine this time dependence for the different solid state processes and compare this with the experimental results. It will be shown that for different solid state processes like free diffusion of implanted deuterium, their surface desorption and formation of metal hydrides lead to distinct values of a and b. Comparison of the experimental values of a and b with the model values can be used to identify the dominant process concurrent during implantation. In untreated copper the surface desorption is inhibited by the prevailing surface contamination and roughness while in polished pure copper surface desorption is very effective. Further, the exponents a and b refer to the asymptotic limits where a steady state is understood to have set in. Thus, before the steady state is attained the behaviour is expected to be different yielding values of a and b different from the model values.

A brief account of the experiments and results in copper and titanium foil specimens is presented in § 2. In § 3 the neutron yield due to d–d fusion is modelled theoretically. The various solid state processes influencing the concentration profile and the corresponding features in neutron yield are discussed in § 4. Finally, the principal results are summarized in § 5.

2. Experiments

2.1 *Details of the experiments*

The deuterium implantations have been carried out using a Sames Model J-15 accelerator. Figure 1 presents a schematic view of the experimental set-up. The stability in beam current and energy was better than 3%. High purity heavy water was electrolysed to produce deuterium gas which was fed into the ion source through a needle valve. The specimens were cut to 2 cm × 2 cm size from polycrystalline foils of titanium and copper. One batch of copper specimens, designated as treated copper, were annealed and polished in order to examine the influence of surface treatment on the results. The foil thickness ranged from 200 to 500 μm. The vacuum in the target chamber was maintained at 10^{-6} mbar by using a turbomolecular pump. The ion beam was focussed to maximize the beam current on the target. Collimators, normally used in ion implantation experiments for defining the ion beam, were avoided in this case to ensure that the deuterons fall only on the specimen. The beam spot had an area of about 1 cm^2. The beam heating was monitored by using a chromel-alumel thermocouple fixed onto the specimen and a temperature rise of about 10 K was observed.

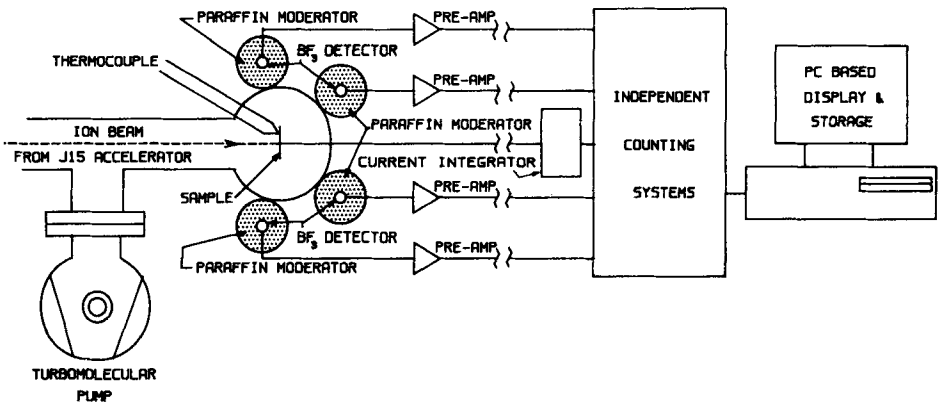

Figure 1. The schematic diagram of the experimental set up.

Neutron counting was performed by using four boron-coated counters along with paraffin moderators placed at a distance of about 30 cm from the specimen. They had independent counting electronics and detector bias set ups. With this arrangement any genuine feature of neutron production should be detected by all the detectors. The performance of the detectors was tested and calibrated using a standard 1 Ci Am–Be source. Background counting over intervals of 300 s was performed for prolonged periods of time before and after the implantation runs and was found to be 4 ± 2 counts in 300 s. Similarly, background counts were taken with the accelerator switched on to deliver a 30 keV, 25 μA proton beam. This did not show any difference from the background counts taken during the machine "off" condition. This confirms that the operation of the RF ion source and the accelerator does not cause noise in the neutron counting set up. The ion source was flushed with deuterium gas for about 4 h before each of the implantation experiments. As a standardization check on the beam quality, the neutron counts obtained during implantation of a virgin copper foil with a 100 keV, 25 μA beam of deuterons were used.

2.2 *The results*

The time of arrival of neutron at each of the detectors was recorded through the communication interrupt of an IBM compatible PC/XT. The neutron counts N as detected by each of the detectors over equal periods of 300 s was obtained by processing the data off-line. These data for copper and titanium specimens were collected at a beam current of 25 ± 1 μA and at 30 ± 1 keV deuterium ion implantation energy. These implantation parameters were chosen so that the specimen does not get overheated during implantation while ensuring sufficient neutron yield for good statistics. Moreover, at these settings the surface effects do not play a dominant role. Figures 2a, b, c show the observed data for copper and titanium respectively.

We observe a close similarity in the qualitative behaviour of the neutron yield data for the two metals. The neutron yield gradually increases with implantation dose. This is due to the accumulation of deuterium in the sample. The general time dependence which is shown as a dotted curve is governed by the deuterium profile which depends on three processes, namely, diffusion, desorption and deuteride formation. This increase is monotonic and analysis of the data shows that it can be

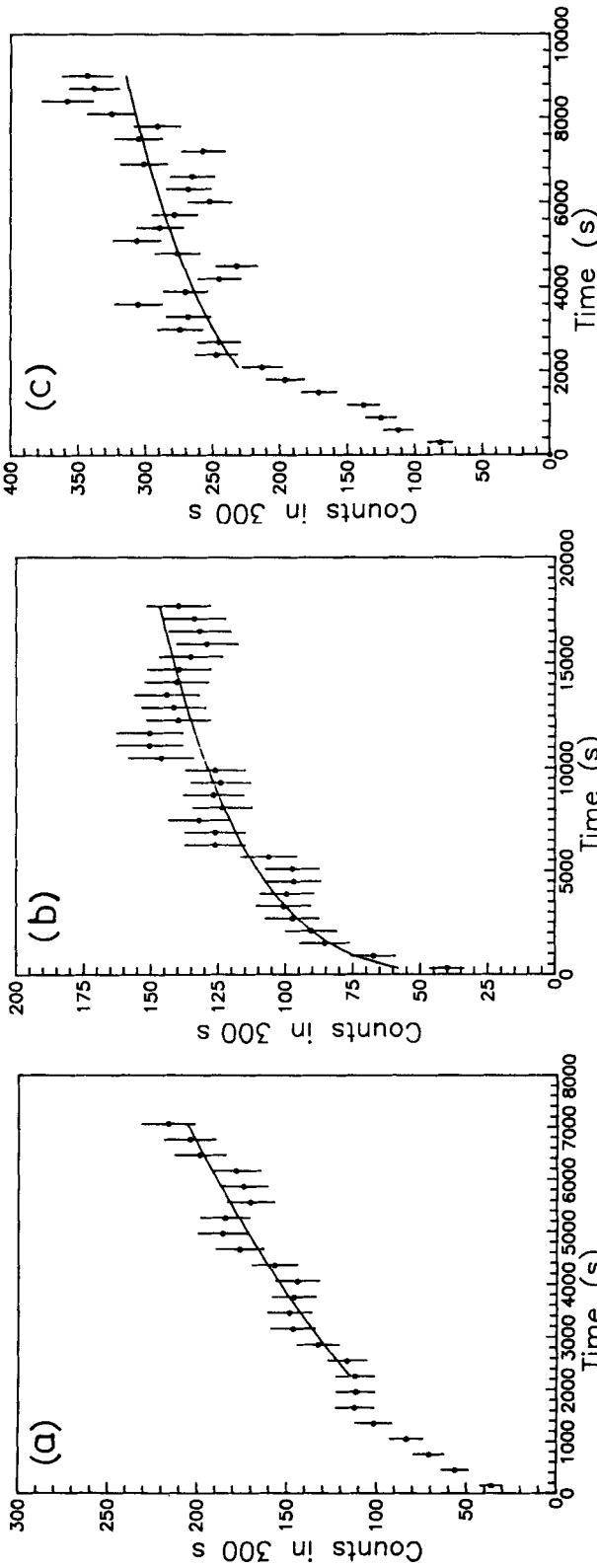

Figure 2. Neutron counts N collected over 300 s as a function of time of deuterium implantation into (**a**) copper, (**b**) titanium and (**c**) treated copper. Ion beam energy $E_0 = 30 \pm 1$ keV, current $I = 25 \pm 1$ μA. Dots (●): Experimental data with error bars and line (—): Fitted asymptotic curve.

Table 1. Values of the exponents a and b for power law fits to the neutron count data.

Material	a	b
Copper	0·5118 ± 0·0395	1·3864 ± 0·0043
Treated copper	0·2103 ± 0·0451	1·3260 ± 0·0134
Titanium	0·2282 ± 0·0240	1·2090 ± 0·0058

fitted to a power law. Over and above this we observe well identified neutron yield peaks. Though these peaks are statistically significant, at this stage the source of their origin is not clear to us. In this paper we will examine the processes which can influence the overall neutron yield curve. As will be shown later, the neutron yield $N(t)$ is expected to show a power law dependence on time asymptotically. Therefore, we make such a fitting of the data to t_m^a (with $t_m = mT$ and $T = 300$ s) and plot the fitted function $N_{asy}(t_m)$ in figure 2 for untreated copper, titanium and treated copper. Similar fitting of the total neutron counts $N_{tot,asy}$ up to time t to a time dependence of the type t^b along with the experimental points have been presented in figure 3. The values of a and b obtained from the experimental data on different materials are tabulated in table 1. The implication of these results will be discussed in the concluding section.

3. Deuterium ion implantation and neutron production by d–d fusion

In this section we discuss the ion implantation condition employed in the present study and make an estimate of the neutron yield behaviour during implantation. Consider a beam of monoenergetic deuterons having an energy E_0 (about 30 keV in the present experiment), incident normal to a plane metal surface at a constant flux J over a beam spot of area A. At time $t = 0$, there is no deuterium in the specimen. As the deuterium beam penetrates the metal it will lose energy and eventually get deposited with a concentration profile $P(x)$ along the depth x. The distribution $P(x)$ arises (Brice 1975) out of multiple scattering of deuterons with the target atoms. $P(x)$ shows a peak at the range $x = R$ and has a straggling S. The values of R and S depend on the incident energy E_0 and the target atom species. This distribution resembles a Gaussian and for convenience of calculation it is taken to be

$$P(x) = [\exp\{-(x-R)^2/(2S^2)\} + \exp\{-(x+R)^2/(2S^2)\}]/\{S\sqrt{(2\pi)}\} \quad (1)$$

for $0 \leqslant x \leqslant \infty$. As the deuterium ions impinge the target already charged with some deuterium, $d(d,n)$ He^3 fusion reaction takes place with a cross section $\sigma(E)$. In the literature, experimental data have been fitted (Duane 1972) to a modified barrier penetration cross section formula

$$\sigma(E) = [A_1/\{1 + (A_2E - A_3)^2\}]/[E.\{\exp(A_4/\sqrt{E}) - 1\}] \quad (2)$$

where $A_1 = (482 \pm 29) \times 10^3$ eV barn, $A_2 = (308 \pm 37) \times 10^{-9}$/eV, $A_3 = 1{\cdot}177 \pm 0{\cdot}077$ and $A_4 = 1514 \pm 13\sqrt{\text{eV}}$. This function fits the experimental data for deuteron

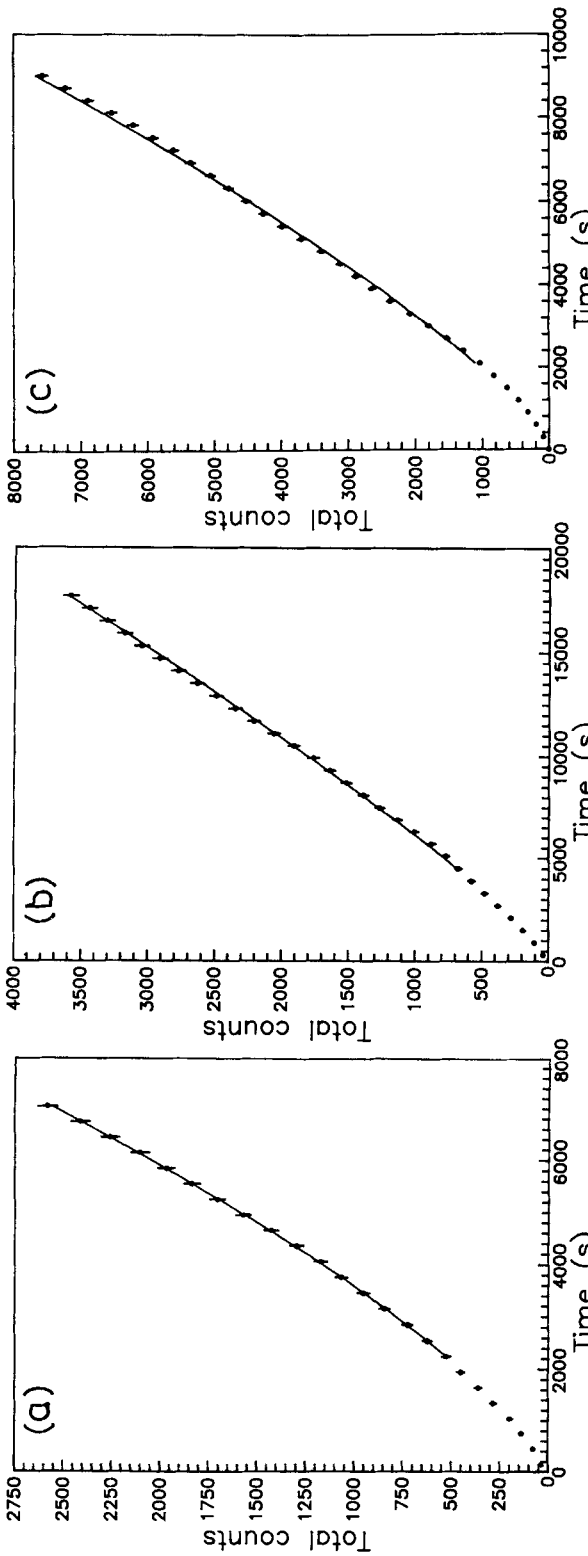

Figure 3. The total neutron counts N_{tot} collected up to time t as a function of time of deuterium implantation into (**a**) copper, (**b**) titanium and (**c**) treated copper. Symbols and ion beam parameters are same as for figure 2.

energies (in eV) in the range of 13·1 keV to 10·2 MeV and is expected to be valid for very low energies as well. However, a simpler function

$$\sigma(E) = k_\sigma E^{5/2} \tag{3}$$

with $k_\sigma = 1{\cdot}7 \times 10^{-7}(\text{keV})^{-5/2}$ barn gives a reasonable fit to the experimental data in the energy range 13·1–30 keV. As the deuterons penetrate the solid metal target, they lose energy (Davisson and Manning 1986) along the depth,

$$\mathrm{d}E/\mathrm{d}x = -(2\sqrt{E_0}/R)E^{1/2}. \tag{4}$$

Thus the energy of the deuterons depends on the depth x as

$$E(x) = E_0(1 - x/R)^2 \tag{5}$$

which implies that the cross section varies along the depth in the specimen. Combining (3) and (5) one gets,

$$\sigma(x) = k_\sigma E_0^{5/2}(1 - x/R)^5. \tag{6}$$

The rate $r(t)$ at which neutrons are produced is given by

$$r(t) = AJ \int_0^R \sigma(x) C(x,t)\,\mathrm{d}x \tag{7}$$

where $C(x,t)$ is the deuterium concentration in the sample. In an experiment, if neutrons are counted over equal intervals of time T, then the counts recorded during $t = mT$ and $(m+1)\,T$ is given by

$$N(mT) = AJ \int_0^R \mathrm{d}x\sigma(x) \int_{mT}^{(m+1)T} C(x,t)\,\mathrm{d}t. \tag{8}$$

Assuming that the deposited deuterium atoms are unable to diffuse and that the metal gets charged continuously without limit, the deuterium concentration is given by

$$C(x,t) = JP(x)t. \tag{9}$$

Using (8) and (9)

$$N(mT) = AJ^2(m + \tfrac{1}{2})\,T^2 k_\sigma E_0^{5/2} F(R) \tag{10}$$

where $F(R)$ is given by

$$\begin{aligned} F(R) = \sqrt{(32/\pi)}\cdot[1 &- (16z^4 + 29z^2/2 + 2)\exp(-z^2) \\ &+ (8z^4 + 9z^2 + 1)\exp(-4z^2) \\ &+ \sqrt{\pi}(16z^5 + 20z^3 + 15z/4)\cdot\{\mathrm{erf}(2z) - \mathrm{erf}(z)\}] \end{aligned}$$

where $z = R/S\sqrt{2}$. Thus the neutron count $N(t_m)$ is expected to rise linearly with time. Similarly, the total neutron yield $N_{\text{tot}}(t)$ up to time t is obtained by performing the t-integration in (8) from 0 to t. The exponents a and b in the asymptotic time dependences of $N(t_m)$ and $N_{\text{tot}}(t)$ are found to be 1 and 2 respectively for this case.

4. Influence of solid state effects on neutron yield

4.1 *Diffusion*

The model developed above is based on the simplified assumption that the implanted deuterons are unable to diffuse. If diffusion is included, equation (9) will no more be valid. In this section we develop a model which allows the diffusion of the deuterium atoms deposited at a rate $JP(x)$. Thus the x and t dependences get coupled by

$$C_{,t} = DC_{,x,x} + JP(x), \quad 0 \leqslant x \leqslant \infty \tag{11a}$$

where $C_{,u}$ is the partial derivative of C with respect to the variable u (for $u = t$ or x) and D is the coefficient of diffusion for deuterium in the metal. The initial and boundary condition of the problem are

$$C(x, 0) = 0 \tag{11b}$$

and

$$C_{,x}|_{x=0} = 0. \tag{11c}$$

The reflecting boundary condition (11c) implies that no gas atom is released by way of desorption at the surface. The solution of equation (11) gives the concentration

$$C(x,t) = J \cdot \int_0^{Dt} \mathrm{d}g\, G \cdot [\exp\{-G^2(x-R)^2/2\} + \exp\{-G^2(x+R)^2/2\}]/D\sqrt{(2\pi)} \tag{12}$$

where $G = (2g + S^2)^{-1/2}$. It may be noted here that the distribution now gets broadened with time because of diffusion. This process ensures transport of deuterium atoms to the near surface regions where the incident ions still have sufficiently high energy for appreciably high cross section for $d(d, n)\,\mathrm{He}^3$ reaction.

This gives rise to a neutron yield rate

$$r(t) = \{ARE_0^{5/2} k_\sigma J^2/D\sqrt{(2\pi)}\} \times \left[d_0(e-S) + \sum_{n=1}^{\infty} (R/2)^{2n}\{(e)^{1-2n} - S^{1-2n}\} d_n/(1-2n) \right] \tag{13}$$

where the coefficients $d_n (n = 0, 1, 2...)$ are given by

$$\begin{aligned} d_n = \{(-1)^n/n!\}[2^{2n+5}\{&2/(2n+1) - 1/(n+1) - 10/(n+1)(2n+3) \\ &- 9/2(n+1)(n+2) + 15/2(n+1)(n+2)(2n+5) \\ &- 2/(n+1)(n+2)(n+3)\} - \{32/(2n+1) - 16/(n+1) \\ &- 40/((n+1)(2n+3) + 29/2(n+1)(n+2) + 15/2(n+1)(n+2)(2n+5) \\ &- 2/(n+1)(n+2)(n+3)\}] \end{aligned}$$

and $e = \sqrt{(2Dt + S^2)}$. The series converges fast and it is evaluated numerically. But for large values of t, the negative powers of t in (13) indicate that the major contribution comes from the first term in (13) which gives the asymptotic limit as

$$r_{\mathrm{asy}}(t) = \{ARk_\sigma J^2 E_0^{5/2}(\pi D)^{-1/2}\} t^{1/2}. \tag{14}$$

The neutron counts recorded during $t = mT$ and $(m + 1)\,T$ is given by

$$N_{asy}(t_m) = \{ARk_\sigma J^2 E_0^{5/2}(\pi D)^{-1/2}\} t_m^{1/2} \tag{15}$$

where $t_m = mT$. The total neutron counts accumulated up to time t is given by

$$N_{tot,asy}(t) = \{2ARk_\sigma J^2 E_0^{5/2}(9\pi D)^{-1/2}\} t^{3/2}. \tag{16}$$

It may be noted from (15) and (16) that the values of a and b in this case are 0·5 and 1·5 respectively.

4.2 *Diffusion followed by desorption*

At the surface of the foil the deuterium concentration C_0 is in equilibrium with the surrounding. As the concentration exceeds C_0 at $x = 0$ desorption takes place and deuterium atoms escape from the metal. In the implantation experiments, which have to be performed in a vacuum chamber, $C_0 \approx 0$. Thus the eventual deuterium concentration $C(0, \infty)$ at the surface will vanish. The concentration $C(x, t)$ is obtained by solving the diffusion equation (11a) along with the initial condition

$$C(x, 0) = 0 \tag{17a}$$

and absorbing boundary condition

$$C(0, t) = 0. \tag{17b}$$

The solution gives

$$C(x,t) = J \cdot \int_0^{Dt} dg\, G \cdot [\exp\{-G^2 \cdot (x-R)^2/2\} - \exp\{-G^2 \cdot (x+R)^2/2\}]/\{D\sqrt{(2\pi)}\}. \tag{18}$$

This will result in a constant asymptotic rate $r_{asy}(t)$ of neutron production and $N_{asy}(mT)$. In this case $N_{tot,asy}(t)$ will be a linear function of time.

An improvement over this can be modelled (Crank 1956) where the concentration gradient at the surface is β times the concentration. This is accomplished by replacing the boundary condition (17b) by

$$C_{,x}|_{x=0} = \beta C(0, t). \tag{19}$$

This gives,

$$\begin{aligned} C(x,t) = J \int_0^{Dt} dg\, G[&\exp\{-G^2(x-R)^2/2\} \\ &+ \exp\{-G^2(x+R)^2/2\}]/\{D\sqrt{(2\pi)}\} - J\beta \int_0^{Dt} dg \exp(\beta^2 g) \\ &\times \int_0^{\infty} dy \exp\{\beta(x+y)\} \operatorname{erfc}\{(2\beta g + x + y)/2\sqrt{g}\} \\ &\times [\exp\{-(y-R)^2/2S^2) + \exp\{-(y+R)^2/2S^2)]/\{DS\sqrt{(2\pi)}\}. \end{aligned} \tag{20}$$

The advantage of this approach can be seen in the fact that the case of reflecting boundary condition (equation 11c) and the case of totally absorbing boundary condition (equation 17b) are obtained from equation (20) as limiting cases with $\beta = 0$ and $\beta = \infty$ respectively. Further, this method is more physical since for small values of t, the concentration at $x = 0$ can be finite as in the practical situation. We, therefore, derive the rate $r(t)$ of neutron yield from (20) as

$$r(t) = \{ARk_\sigma J^2 E_0^{5/2}/D\}\left[\sum_{n=0}^{\infty}(R/2)^{2n}\{(\sqrt{e})^{1-2n} - S^{1-2n}\}\,d_n/(1-2n)\sqrt{(2\pi)}\right.$$

$$\left. - 120\sum_{j=0}^{\infty}(-1)^j q_j(t)\right] \tag{21}$$

where $q_j(t)$ is given by the inverse Laplace transform

$$q_j(t) = L^{-1}[\{s^{(j+3)/2}\beta/(\beta+\sqrt{s})\}\sum_{m=0}^{j} M_m R^{j-m}/(j-m+6)!,$$

$$M_m = \int_0^\infty dy\, y^m [\exp\{-(y-R)^2/2S^2\} + \exp\{-(y+R)^2/2S^2\}]/S\sqrt{2\pi}$$

and $d_n (n = 0, 1, 2...)$ are as defined in (13). The asymptotic form of (21) leads to the eventual time dependences as given by

$$r_{asy}(t) = ARk_\sigma J^2 E_0^{5/2}/6D\beta, \tag{22}$$

$$N_{asy}(t_m) = ARTk_\sigma J^2 E_0^{5/2}/6D\beta \tag{23}$$

and

$$N_{tot,asy}(t) = (ARk_\sigma J^2 E_0^{5/2}/6D\beta)t. \tag{24}$$

It may be noted from (22) that the asymptotic rate $r(t)$ of neutron yield is independent of t. Similarly, asymptotically the neutron production $N(t_m)$ during $t = mT$ and $t = (m+1)T$ is independent of t_m as seen in (23). And the eventual total accumulated neutron counts up to time t is a linear function of time. This model predicts the values of a and b to be 0 and 1 respectively. Different values of the parameter β of this model correspond to different degrees of desorption. $\beta = 0$ corresponds to no desorption leading to a reflecting boundary condition of equation (11c) and $\beta = \infty$ results in a totally absorbing boundary condition of equation (17b). And an intermediate value of β will influence the time required for the asymptotic behavior to be observed. This aspect will be discussed in a subsequent section.

4.3 *Diffusion hindered by formation of hydride*

Only the free deuterium atoms are capable of diffusing. But, as the implanted deuterium concentration builds up, a part of these deuterium atoms can get chemically bound to the metal lattice in the form of hydrides. The extent to which this effect can take place depends on the chemical nature of the metal and the stability of their hydrides. For example, titanium forms its stable hydrides readily, whereas the copper hydride hardly forms. Once the hydride is formed, the associated deuterium is no more free to diffuse. On the other hand, if the deuterium concentration builds up locally by way of diffusion of the free deuterium atoms a part of it can subsequently get immobilized by formation of hydride. Thus, at any instant of time the concentration

profile $C(x,t)$ is composed of two parts; the mobile component $C_m(x,t)$ and the immobile component $C_h(x,t)$ where

$$C(x,t) = C_m(x,t) + C_h(x,t). \tag{25}$$

The mobile component $C_m(x,t)$ obeys,

$$C_{m,t} = DC_{m,x,x} - kC_m + JP(x) \tag{26}$$

along with the boundary condition (11c). Here k denotes the fraction of the deuterium concentration that gets immobilized by the formation of deuterides. The reflecting boundary condition has been used in order to examine the effect of hydride formation independent of the surface desorption. Equation (26), when solved, gives

$$C_m(x,t) = J\int_0^{Dt} dg\, G\exp(-kg/D)[\exp\{-G^2(x-R)^2/2\} + \exp\{-G^2(x+R)^2/2\}]/\{D\sqrt{(2\pi)}\}. \tag{27}$$

The immobile part $C_h(x,t)$ follows

$$C_{h,t} = k\cdot C_m(x,t). \tag{28}$$

Using (27) for $C_m(x,t)$, equation (28) is solved to obtain

$$C_h(x,t) = C_m(x,t)kt - kJ\int_0^{Dt} dg\, G\exp(-kg/D)[\exp\{-G^2(x-R)^2/2\} + \exp\{-G^2(x+R)^2/2\}]/D\sqrt{(2\pi)}. \tag{29}$$

And the total deuterium concentration can be obtained by using (27) and (29) in (25). In order to examine the asymptotic time dependences it is convenient to use the Laplace transform of $C(x,t)$ given by

$$\tilde{C}(x,s) = Q(s)/s^2 \tag{30}$$

where the function $Q(s)$ is written as

$$Q(s) = J(k+s)^{1/2}\int_0^{\infty} dy P(y)[\exp\{-(k+s)^{1/2}|x-y|\} + \exp\{-(k+s)^{1/2}|x+y|\}]/2D.$$

where the source function P is defined in (2). By using an appropriate Tauberian theorem (Feller 1977) it can be shown that for large time

$$C(x,t) = tQ(1/t) \approx t\cdot Q(0). \tag{31}$$

Such a linear time dependence of $C(x,t)$ leads to a linear time dependence of $r_{asy}(t)$ and $N_{asy}(t_m)$ as

$$r_{asy}(t) = K_h t \tag{32}$$

and

$$N_{asy}(t_m) = K_h t_m \tag{33}$$

where K_h is a constant. The asymptotic behavior of the total neutron counts up to time t is given by

$$N_{\text{tot,asy}}(t) = (K_h/2)t^2. \tag{34}$$

Thus, in the case where hydride formation takes place concurrent with implantation, a and b take values 1 and 2 respectively. Similar asymptotic behavior can be obtained even when deuterium gas is desorbed.

The asymptotic time dependences seen in these models are to be compared with the experimental results and a discussion of this is presented in the next section.

5. Summary

Assuming a relatively simple energy dependence of the d–d fusion cross section to be valid in a limited energy range, the neutron yield characteristics during deuterium implantation have been evaluated theoretically for different solid state processes that might take place during implantation. The asymptotic time dependence of the neutron counts during 300 s intervals and of the total neutron counts have been found to be of the type t_m^a and t^b respectively with estimates of a and b tabulated in table 2.

The experimental values of a and b for copper are $0{\cdot}5118 \pm 0{\cdot}0395$ and $1{\cdot}3864 \pm 0{\cdot}0043$ respectively (see table 1). These are very close to 0·5 and 1·5 respectively indicating that in copper the implantation profile gets broadened by diffusion, copper hydride is not formed during implantation and the implanted deuterium does not escape the specimen by desorption. Such a case is characterized by $\beta = 0$ and the asymptotic limit is attained after a time of the order of R^2/D. This is at variance with earlier observations (Besenbacher *et al* 1984) where it is noted that the implanted deuterium desorbs out at the surface. Anyway, the implanted atoms do diffuse to the sub-surface region but the effectiveness of desorption depends (Wilson *et al* 1987) on the surface condition and possible presence of defects in the region to act as hydrogen traps. For example, if the specimens are not annealed and polished after cold rolling to the required thickness, as in the case of the untreated copper specimens mentioned above, desorption is most likely to be inhibited. In order to examine this aspect another set of high purity annealed and polished copper specimens were used. The exponents a and b for these specimens, presented in table 1 against treated copper, are found to be $0{\cdot}2103 \pm 0{\cdot}0451$ and $1{\cdot}3260 \pm 0{\cdot}0134$ respectively which are similar to the case of titanium where the exponents a and b are $0{\cdot}2282 \pm 0{\cdot}0240$ and $1{\cdot}2090 \pm 0{\cdot}0058$ respectively. From this it may be inferred that the implanted deuterium profile in titanium is influenced by both diffusion and desorption; however, the asymptotic state

Table 2. Theoretical estimates of a and b in different model calculations.

Model	a	b
No diffusion	1	2
Free diffusion	0·5	1·5
Diffusion and desorption	0	1
Diffusion hindered by formation of hydrides	1	2

has not yet been attained. The deuterium atoms are transported by diffusion from the implanted region to the surface where a part of them escapes. The asymptotic steady state under continuous implantation, diffusion and desorption is attained only after a time of the order of $1/\beta^2 D$. A lower limit for β can be obtained by comparing this with the time R^2/D for asymptotic behavior to be achieved with diffusion and no loss by desorption. Desorption plays an important role when $1/\beta^2 D < R^2/D$ (i.e. $\beta > 1/R$). In this case, during the period earlier to $t = 1/\beta^2 D$ since the asymptotic regime has not yet been reached, a might appear to take an intermediate value between 0 and 0·5 and b between 1 and 1·5 as has been observed in the experiments using titanium and treated copper specimens (see table 1). If hydrides were to form during implantation, the exponents were expected to take higher values ($a = 1$ and $b = 2$). Although the hydrides of titanium are known to be stable under equilibrium conditions, the comparatively lower experimental values of a and b indicate that there is no tendency for formation of hydrides during deuterium implantation even in a narrow zone of the specimen around the peak of the implantation profile where the concentration is the highest. In copper the hydrides are anyway not stable. In titanium the hydrides do not form during implantation probably because the average energy of the implanted deuterium ions at the depth around R is still about 125 eV when they can no more displace lattice atoms. This terminal energy, therefore, has to be dissipated in the specimen near R where the ions eventually come to rest. Because the dimensions of the specimens are small, the thermal steady state is attained soon after the implantation starts. In the steady state the temperature of this zone has been estimated (Rubia *et al* 1989) for some typical materials and implantation conditions, and is seen to be very much higher than the temperature where the hydrides decompose. In titanium the hydrides decompose at about 600°C (Mark *et al* 1978). And in copper the hydride is unstable even at ambient temperature.

In the above we have not analysed the possibility of deutride formation in a region away from the peak of implantation profile. Pontau *et al* (1980) and Roth *et al* (1980) have reported that deutride layer in Ti forms first near the surface and not at the peak of the implantation profile in agreement with our discussion above. They have also reported the inward growth of the deuteride layer. Although we have not done the detailed analysis of the kinetics of this case it appears that the neutron counts in the asymptotic limit may exhibit similar behavior to the case presented above where the disorption guides the kinetics.

In figure 2, where the experimental neutron counts collected during 300 s intervals are plotted against time, there are large deviations from the average trend. These features of the data appear in the form of peaks of neutron counts in time. These peak heights are much larger than the errors normally encountered in counting experiments. The origin of these peaks is not definitely known; but they cannot be expected to arise from the known mechanisms discussed in this paper.

References

Alefeld G and Volkl J (eds) 1978 *Hydrogen in metals* (Berlin: Springer Verlag) Vol. I and II
Besenbacher E, Bech Nielsen B and Myers S M 1984 *J. Appl. Phys.* **56** 3384
Brice D K 1975 *Ion implantation range and energy deposition distributions* (New York: IFI/Plenum Press)
Crank J 1956 *The mathematics of diffusion* (London: Oxford University) p. 124
Davisson C M and Manning I 1986 NRL report no. 8859 p. 2

Diaz de la Rubia T, Averback R S and Hsieh H 1989 *J. Mater. Res.* **4** 579
Duane B H 1972 BNWL report no. 1685 p. 75
Feller W 1977 in *An introduction to probability theory and its applications* (New Delhi: Wiley Eastern) p. 418
Jones S E, Palmer E P, Czirr J B, Decker D L, Jensen G L, Thorne J M, Taylor S F and Rafelski J 1989 *Nature* (*London*) **338** 737
Mark H F, Othmer D F, Overberger C G and Seaborg G T (eds) 1978 *Encyclopedia of chemical technology* (New York: Wiley) **Vol. 12** p. 777
Mueller W M 1968 in *Metal hydrides* (New York: Academic Press)
Pontau A E, Wilson K L, Greulich F and Haggmark L G 1980 *J. Nucl. Mater.* **91** 343
Roth J, Eckstein W and Bohdansky J 1980 *Radiat. Effects* **48** 231
Srinivasan M 1991 *Curr. Sci.* **60(7)** 417
Wilson K L, Causey R A, Baskes M I and Kamperschroor J 1987 *J. Vac. Sci. Technol.* **A5** 2319